

Characterization of Polymerized Layer of Alkylsilane on Surfaces of Silica Filler Materials by Force Spectroscopic Measurements Using Atomic Force Microscope

Yuki Arai^{1*} and Tomohiro Hayashi^{2**}

¹Advanced Technology Research and Development Center, Research and Innovation Promotion Headquarters, Showa Denko Materials Co. Ltd., 13-1 Higashi-cho 4 chome, Hitachi-shi, Ibaraki 317-8555, Japan

²Department of Materials Science and Engineering, School of Materials and Chemical Technology, Tokyo Institute of Technology, 4259 Nagatsuta-cho, Midori-ku, Yokohama 226-8502, Japan

(Received September 14, 2022; accepted September 26, 2022)

Keywords: silica filler, force spectroscopy, atomic force microscopy, alkylsilane, polymer film

We demonstrated the characterization of silica filler materials by force spectroscopic measurements using an atomic force microscope. Our measurement revealed the local thickness distribution of a film of polymerized alkylsilane around silica colloids at nanometer resolution. In addition, our method enabled us to monitor the changes in the thickness distribution after chemical treatment of the materials. These findings cannot be obtained with other popular surface analytical techniques such as X-ray photoelectron spectroscopy and scanning electron microscopy. Our analytical approach is expected to contribute to the evaluation of local distributions of polymeric materials and nanoparticles and to the design of new filler materials in the future.

1. Introduction

Filler materials are essential materials used in semiconductor devices.^(1,2) The functions of filler materials in packaging devices include the passivation of integrated circuits, enhancement of mechanical stiffness (stability), improvement of heat conductivity for heat dissipation, and insulation.^(3–7) Recent filler materials used for the passivation of electric devices have been composites of micro- or nanoparticles (mainly silica) and polymeric materials. By changing the proportion of their combination, we can optimize the functions.

Despite the intensive use of nanocomposite silica nanoparticles and polymers in the semiconductor industry, the distribution of silica nanoparticles, the polymer matrix, and their interface have not been examined in detail. However, these issues directly affect the functions mentioned above. Figure 1 shows scanning electron microscopy (SEM) (JSM-IT100, JEOL, Tokyo, Japan) images of silica particles with and without a polymer matrix. From this result, it is difficult to discuss the interfacial properties of the silica/polymer composite. Figure 2 displays the X-ray photoelectron spectra (K-ALPHA+, Thermo Fisher Scientific, MA, United States) of composites and bare silica particles. In addition to the signal from Si2p, we observed a strong

*Corresponding author: e-mail: arai.yuki.xicon@showadenko.com

**Corresponding author: e-mail: tomo@mac.titech.ac.jp

<https://doi.org/10.18494/SAM4101>

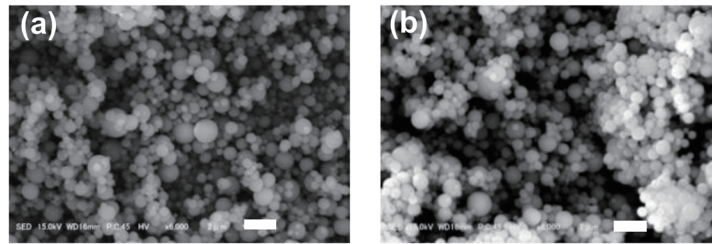


Fig. 1. SEM images of (a) bare silica particles and (b) silica particles processed with epoxy silane. The scale bars correspond to 2 μm .

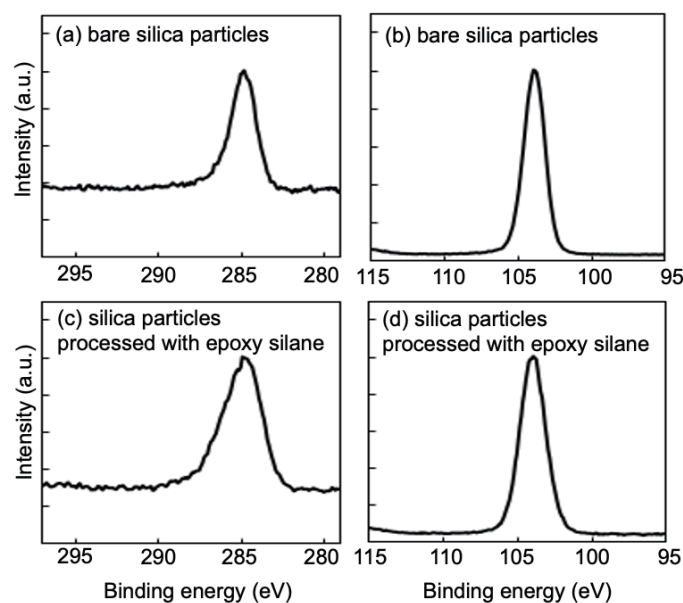


Fig. 2. XPS spectra of (a) C1s and (b) Si2p regions measured for (c) bare silica particles, and (d) for silica-polymer composites.

C1s signal from both samples. X-ray photon spectroscopy (XPS), the most widely used surface-sensitive analytical tool, cannot distinguish between surfactants for protection and carbon contaminants from the C1s signals from the silica particles. The thicknesses of polymer films coated on flat solid surfaces can be evaluated by ellipsometry, X-ray, and neutron reflectivity measurements.^(8,9) Different from the cases of flat surfaces, we cannot apply these analytical techniques to evaluate the distribution of the polymer matrix. To summarize, we cannot investigate the distribution of organic materials constituting silica filler materials by conventional analytical techniques.

In this work, we propose a method for exploring silica/polymer interfaces using atomic force microscopy (AFM). The local surface mechanical properties have been studied by AFM.⁽¹⁰⁾ However, the distribution of the polymer matrices around the silica colloids has not been elucidated. Force–separation measurement using AFM enables us to measure the thickness of

polymeric materials by pressing the probe tip into the polymer matrix.^(11–15) By this approach, we attempt to acquire a cross-sectional view of the silica/polymer interface by mapping the force–separation curves. On this basis, we attempt to visualize the distribution of the polymer matrix around the silica particles for the first time.

2. Materials and Methods

In this work, we analyzed two types of commercial silica fillers. One comprised bare silica particles (SO-25 H/24C, mean diameter of 500 nm, Admatechs Co., Miyoshi-shi, Japan). The other comprised silica particles covered with polymerized epoxy (SE2200-SEJ, SO-25 treated with 3-glycidoxypropyltrimethoxysilane, Admatechs Co.).

We used a commercial AFM system (SPM8100, Shimadzu, Kyoto, Japan). The spring constants of Si_3N_4 cantilevers (PB800PSA-A, nominal spring constant of 0.15 nN/nm, Olympus, Tokyo, Japan) were calibrated by a thermal noise method.⁽¹⁶⁾ The separation at the origin (separation = 0) was defined as the point where the probe in contact with the hard surface exhibited a linear increase in force as a function of the z-piezo displacement in the AFM system.^(17–19) Before force-separation curve mapping, we performed rough 2D mapping with a small triggering force (<300 pN) to obtain the topography of the silica colloid surfaces. Then, we performed mapping along a line with a higher triggering force (1.5 nN). Force–separation curve measurements were performed at 62×3 points in an area of $200 \times 25 \text{ nm}^2$. All the measurements were performed in NaCl solution (10 mM) to suppress electrostatic double layer repulsion and strong adhesion between the polymer matrix and AFM probe.

3. Results and Discussion

Figure 3 shows typical force–separation curves recorded with the approach (black) and release (red) of the probe. The curves for the approach and release observed for a bare silica particle are almost identical [Fig. 3(a)]. At a separation below 10 nm, we observed weak

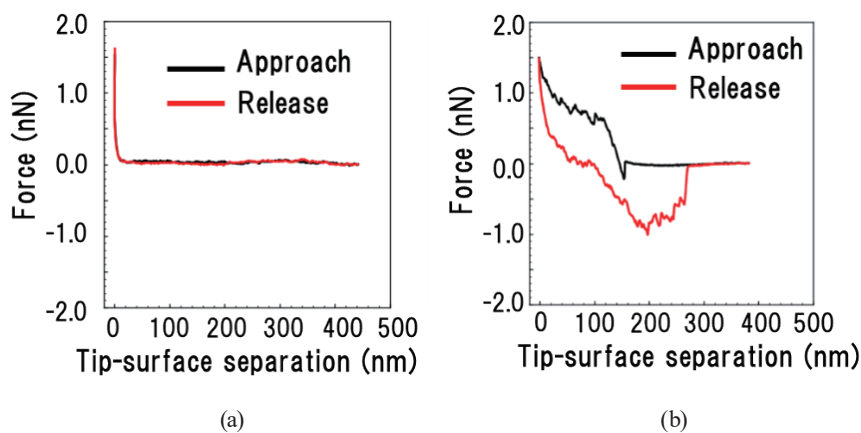


Fig. 3. (Color online) Force–separation curves recorded on approach (black) and release measured with (a) bare silica particle and (b) silica–polymer composite.

compression (nonlinear behavior of the force–separation curve). We consider this to be due to the surfactant and/or contaminants on the silica particle, which was confirmed by XPS [Fig. 2(a)]. When the probe reached the surface, the force increased abruptly. We also observed no adhesion between the silica colloid and probe, indicating that no bridging occurred between the probe and the silica surface upon the retraction of the probe.

In contrast, the shapes of the force–separation curves are completely different for the silica–polymer composite [Fig.3(b)]. We observed a dip upon contact of the probe to the substrate at around 150 nm in the approach curve, most probably due to van der Waals attraction. The probe penetrated a relatively hard layer after the dip, and yielding of the polymer layer was observed. This result indicates that a relatively mechanically stable layer was formed at the surface. We consider that water molecules generated by the cross-linking reaction may easily escape from the layer at the polymer surface, resulting in the high degree of cross-linking in the polymer layer. After the penetration of the probe tip into the layer, the yielding force was observed during indentation by the probe, indicating that the layer beneath the surface was soft. With the retraction of the tip, the curve does not follow the approach curve, resulting in hysteresis between the approach and retraction curves, indicating plastic deformation of the polymer matrix.

As discussed above, the force–separation curve measurements reveal the distribution of the polymer matrix covering the silica particles. Therefore, the mapping of force curves can be used to visualize the 3D distribution of the polymer matrix. By mapping the force acting on the probe during its approach, we can visualize the distribution of the polymer matrix around the silica particles [Figs. 4(a) and 4(b)]. The force–separation curves recorded with a bare silica particle revealed the accumulation of surfactants and/or contaminants with a constant thickness of a few nm.

On the other hand, for the silica–polymer composites, we confirmed that a polymer layer with a thickness ranging from 50 to 100 nm had formed on a silica sphere. We can evaluate not only the local thickness but also the local distribution of the elastic modulus, which strongly depends on the cross-linking degree of the epoxy silane molecules. Note that there is a small

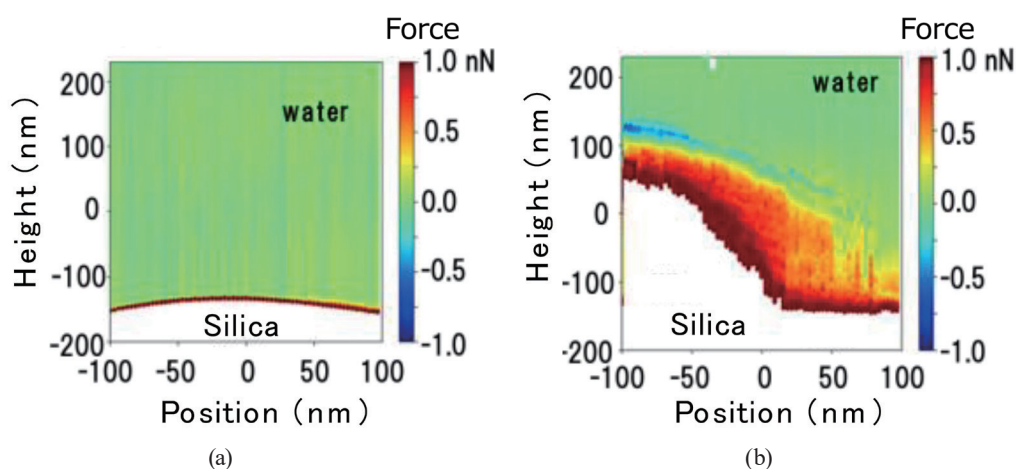


Fig. 4. (Color online) Distribution of force recorded on approach of probe evaluated on (a) bare silica particle and (b) silica–polymer composite.

discrepancy between the force distribution in the first and second scans (Fig. 5), indicating a mechanical effect on the polymer matrix by force mapping. Therefore, the mechanical properties of the polymer matrix should be evaluated from the results of the first force mapping.

This force-mapping method can also follow changes in the polymer matrix after physical or chemical treatment. Figure 6 displays the results of force mapping of the silica–polymer composite after rinsing with chloroform. As shown, no polymer layer was observed. This indicates that the polymer matrix was not immobilized to the silica particles via covalent bonds. In this work, the silane molecules reacted with silanol groups on the particle surfaces and formed a monolayer. The surrounding molecules did not form covalent bonds with the molecules constituting the monolayer. Therefore, the polymer matrix was easily removed by rinsing, even

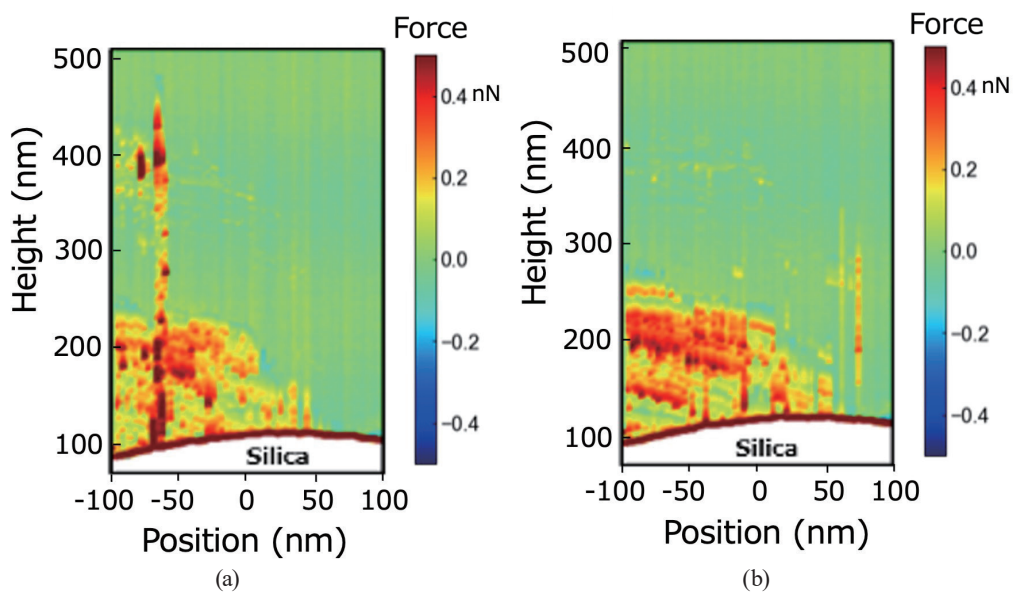


Fig. 5. (Color online) Distribution of force recorded on approach of probe evaluated with silica–polymer composites in (a) first and (b) second scans.

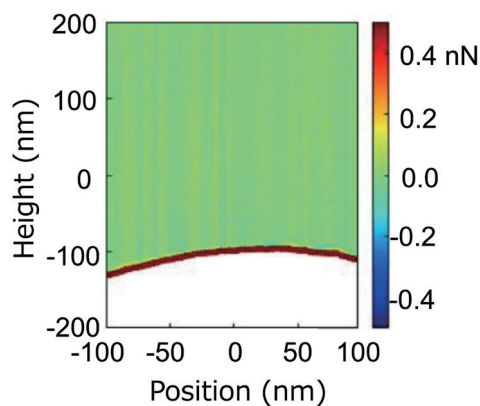


Fig. 6. (Color online) Distribution of force recorded on approach of probe evaluated with silica–polymer composite after rinsing with chloroform.

though the surrounding molecules were cross-linked. Such an interfacial property significantly affects the mechanical and heat transport properties of silica–polymer composites.⁽²⁰⁾ Therefore, the analysis using force mapping is expected to be beneficial for optimizing the experimental conditions and choice of materials.

4. Conclusions

We performed mappings of force–separation curves using an AFM to investigate the interfacial properties of silica–polymer composites. The measurement revealed the distribution of a polymer layer around the silica particles, enabling us to evaluate the local thickness of the polymer layer. We also demonstrated that the force-mapping method can characterize changes in the distribution resulting from physical and chemical processes acting on the composites. In general, silica–polymer composites have been analyzed by XPS, SEM, thermogravimetry, and IR absorption spectroscopy. However, no method has succeeded in the visualization and evaluation of the local distribution of a polymer layer around particles. We strongly believe that the proposed method will contribute to the analysis of filler materials used in various industrial applications.

Acknowledgments

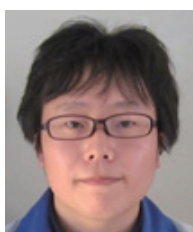
We thank Ms. Kazue Taki for the administration of this project. This work was supported by JSPS KAKENHI grants (Grant Numbers JP22H04530, JP21H05511, JP20H05210, and JP19H02565) and performed under the “Five-star Alliance” Research Program in “NJRC Mater. & Dev.”

References

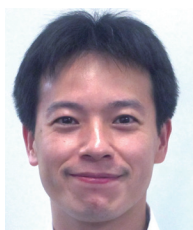
- 1 J. S. Meth, S. G. Zane, C. Chi, J. D. Londono, B. A. Wood, P. Cotts, M. Keating, W. Guise, and S. Weigand: *Macromolecules* **44** (2011) 8301. <https://doi.org/10.1021/ma201714u>
- 2 D. W. Lee and B. R. Yoo: *J. Ind. Eng. Chem.* **38** (2016) 1. <https://doi.org/10.1016/j.jiec.2016.04.016>
- 3 M. Ohashi, S. Kawakami, Y. Yokogawa, and G.-C. Lai: *J. Am. Ceram. Soc.* **88** (2005) 2615. <https://doi.org/10.1111/j.1551-2916.2005.00456.x>
- 4 P. L. Teh, M. Jaafar, H. M. Akil, K. N. Seetharamu, A. N. R. Wagiman, and K. S. Beh: *Polym. Adv. Technol.* **19** (2008) 308. <https://doi.org/10.1002/pat.1014>
- 5 P. L. Teh, M. Mariatti, H. M. Akil, C. K. Yeoh, K. N. Seetharamu, A. N. R. Wagiman, and K. S. Beh: *Mater. Lett.* **61** (2007) 2156. <https://doi.org/10.1016/j.matlet.2006.08.036>
- 6 R. Yan, F. Su, L. Zhang, and C. Z. Li: *Composites, Part A* **125** (2019). <https://doi.org/10.1016/j.compositesa.2019.105496>
- 7 A. Guyard, J. Persello, J. P. Boisvert, and B. Cabane: *J. Polym. Sci., Part B: Polym. Phys.* **44** (2006) 1134. <https://doi.org/10.1002/polb.20768>
- 8 E. Chason and T. M. Mayer: *Crit. Rev. Solid State Mater. Sci.* **22** (1997) 1. <https://doi.org/10.1080/10408439708241258>
- 9 R. Inoue, K. Kawashima, K. Matsui, M. Nakamura, K. Nishida, T. Kanaya, and N. L. Yamada: *Phys. Rev. E* **84** (2011). <https://doi.org/10.1103/PhysRevE.84.031802>
- 10 D. M. Huang and D. Chandler: *Proc. Natl. Acad. Sci. U.S.A.* **97** (2000) 8324. <https://doi.org/10.1073/pnas.120176397>
- 11 I. Argatov, F. M. Borodich, and X. Q. Jin: *Front. Mech. Eng.* **8** (2022). <https://doi.org/10.3389/fmech.2022.931271>
- 12 N. P. Huynh, T. E. Le, and K. H. Chung: *Microsc. Microanal.* **27** (2021) 1488. <https://doi.org/10.1017/S143192762101285x>

- 13 J. Czajor, W. Abuillan, D.-V. Nguyen, C. Heidebrecht, E. A. Mondarte, O. Kononov, T. Hayashi, D. Felder-Flesch, S. Kaufmann, and M. Tanaka: RSC Adv. **11** (2021) 17727. <https://doi.org/10.1039/D1RA02571F>
- 14 K. Takano, T. Nyu, T. Maekawa, T. Seki, R. Nakatani, T. Komamura, T. Hayakawa, and T. Hayashi: RSC Adv. **10** (2019) 70. <https://doi.org/10.1039/c9ra09043f>
- 15 E. A. Q. Mondarte, H. Tahara, K. Suthiwanich, S. Song, F. Wang, and T. Hayashi: Sens. Mater. **33** (2021) 223. <https://doi.org/10.18494/sam.2021.3069>
- 16 J. L. Hutter and J. Bechhoefer: Rev. Sci. Instrum. **64** (1993) 1868. <https://doi.org/10.1063/1.1143970>
- 17 H.-J. Butt, B. Cappella, and M. Kappl: Surf. Sci. Rep. **59** (2005) 1. <https://doi.org/10.1016/j.surfrep.2005.08.003>
- 18 T. Hayashi, Y. Tanaka, Y. Koide, M. Tanaka, and M. Hara: Phys. Chem. Chem. Phys. **14** (2012) 10196. <https://doi.org/10.1039/c2cp41236e>
- 19 T. Sekine, Y. Tanaka, C. Sato, M. Tanaka, and T. Hayashi: Langmuir **31** (2015) 7100. <https://doi.org/10.1021/acs.langmuir.5b01216>
- 20 K. Gaska, A. Rybak, C. Kapusta, R. Sekula, and A. Siwek: Polym. Adv. Technol. **26** (2015) 26. <https://doi.org/10.1002/pat.3414>

About the Authors



Yuki Arai received his M.S. degree from Tokyo Institute of Technology in 2010. His master's thesis was on imaging techniques using scanning probe microscopy. From 2010 to 2017, he developed rechargeable batteries in a battery manufacturing company in Japan. He joined Showa Denko Materials (formerly Hitachi Chemical) in 2017 and was promoted to assistant manager in 2022. His research interests are in analytical chemistry, functional materials, and chemoinformatics. (arai.yuki.xicon@showadenko.com)



Tomohiro Hayashi received his Ph.D. degree in 2003 from Ruprecht-Karls-Universität Heidelberg. He joined Tokyo Institute of Technology in 2003 as a postdoc and became an associate professor in 2010. His specialties are surface and interface science, scanning probe microscopy, materials informatics, and computer simulations. He has been awarded 11 academic prizes, including the Asahi Kasei award of the Society of Polymer Science, Japan (2011). His activities are summarized at <http://lab.spm.jp/>. (tomo@mac.titech.ac.jp)

